Photochemistry and Photobiology, 2017, 93: 805–814

Integration of Temperature and Blue-Light Sensing in *Acinetobacter baumannii* Through the BlsA Sensor†

Inés Abatedaga[1], Lorena Valle[1,‡], Adrián E. Golic[2,‡], Gabriela L. Müller[2], Matías Cabruja[3], Faustino E. Morán Vieyra[1], Paula C. Jaime[1], María Alejandra Mussi[2]* and Claudio D. Borsarelli[1]*

[1]Instituto de Bionanotecnología del NOA (INBIONATEC), Universidad Nacional de Santiago del Estero (UNSE), CONICET, Santiago del Estero, Argentina
[2]Centro de Estudios Fotosintéticos y Bioquímicos (CEFOBI-CONICET), Universidad Nacional de Rosario (UNR), Rosario, Argentina
[3]Instituto de Biología Molecular y Celular de Rosario (IBR-CONICET), Universidad Nacional de Rosario (UNR), Rosario, Argentina

Received 3 December 2016, accepted 17 February 2017, DOI: 10.1111/php.12760

ABSTRACT

BlsA is a BLUF photoreceptor present in *Acinetobacter baumannii*, responsible for modulation of motility, biofilm formation and virulence by light. In this work, we have combined physiological and biophysical evidences to begin to understand the basis of the differential photoregulation observed as a function of temperature. Indeed, we show that *blsA* expression is reduced at 37°C, which correlates with negligible photoreceptor levels in the cells, likely accounting for absence of photoregulation at this temperature. Another point of control occurs on the functionality of the BlsA photocycle itself at different temperatures, which occurs with an average quantum yield of photoactivation of the signaling state of 0.20 ± 0.03 at $15°C < T < 25°C$, but is practically inoperative at $T > 30°C$, as a result of conformational changes produced in the nanocavity of FAD. This effect would be important when the photoreceptor is already present in the cell to avoid almost instantaneously further signaling process when it is no longer necessary, for example under circumstances of temperature changes possibly faced by the bacteria. This complex interplay between light and temperature would provide the bacteria clues of environmental location and dictate/modulate light photosensing in *A. baumannii*.

INTRODUCTION

Acinetobacter baumannii is a threatening human pathogen that shows a peculiar ability to persist in the hospital environment and acquire resistance determinants (1). This microorganism is able to sense and respond to blue light, modulating important aspects related to its pathogenicity such as motility, biofilm formation and virulence against *Candida albicans*, as has been shown for the first time by some members of our group (2). These responses depend on the only photoreceptor encoded in the *A. baumannii* genome, which belongs to the blue-light sensing using flavin (BLUF) type, and which was designated BlsA (2). Indeed, blue-light absorption in the dark state (dBlsA), referred to as the dark-adapted conformation of the photoreceptor, triggers a photocycle to yield the signaling state (sBlsA), which typically shows a ~10–12 nm red-shift of the absorption band indicating that BlsA is an active photoreceptor (2). The photocycle of dBlsA was later studied by ultra-fast time-resolved infrared (TRIR) spectroscopy, and it was shown that the signaling state of sBlsA is directly populated from the S_1 excited state of FAD in few ps (3). The formation of the signaling state of BLUFs occurs in the subnanosecond regime, and nowadays it is accepted that the ultra-short lifetime of the S_1 state together with low fluorescence quantum yield (<0.01) are a consequence of a prompt electron-transfer (ET) process from a nearby Tyr residue (4–12). For instance, femtosecond transient absorption spectroscopy to the Slr1694 BLUF domain of *Synechocystis PCC6803* demonstrated the transient intermediacy of the expected ET primary product FAD radical anion ($FAD^{\cdot-}$), followed by the formation of the neutral flavin semiquinone FADH radical ($FADH^{\cdot}$) indicating that subsequent proton transfer can also take place (6). This prompt charge-transfer modification of FAD in the BLUF proteins is responsible of the observed red-shift in the absorption band of the signaling state, due to hydrogen-bonding rearrangement involving the isoalloxazine ring of FAD and highly conserved residues Gln and Tyr in the active site (Fig. 1) (6,10–14).

The surprising fact is that in the signaling state of BLUFs, the FAD undergoes subtle structural rearrangements but strong enough to trigger a significant change of the protein conformation for signal transduction (7,12). For BlsA, the β5 strand containing the N-terminal residue Trp92 was proposed to move upon light-induced formation of sBlsA, initiating the biological signal transduction probably by formation of a complex with the downstream target protein (3). After photoactivation, the signaling state of BLUFs relaxes back in the time window of few seconds to several minutes depending on the protein (2,3,5,6,12), suggesting that moderate to large thermal activation is required.

An intriguing and still not much explored aspect is that blue-light photoregulation depends on temperature in *A. baumannii*, occurring at 24°C but not at 37°C, and therefore posing the

*Corresponding authors' e-mails: cdborsarelli@gmail.com (Claudio D. Borsarelli); mussi@cefobi-conicet.gov.ar (María Alejandra Mussi)
†This article is a part of the Special Issue dedicated to Dr. Wolfgang Gärtner on the occasion of his 65th birthday.
‡These authors contributed equally to this work.

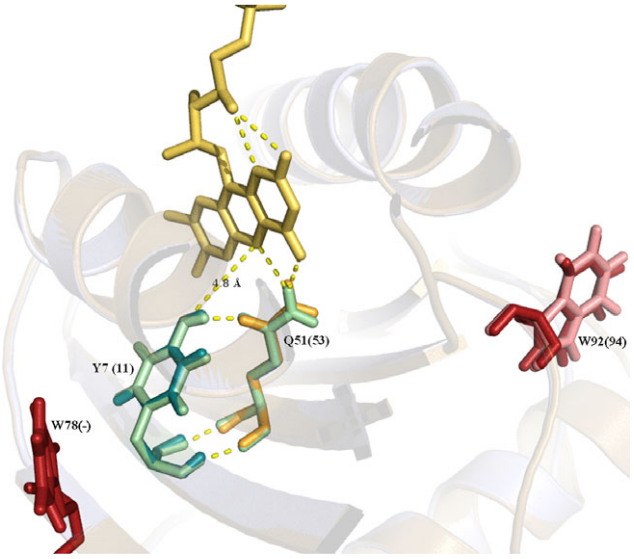

Figure 1. Structure of Slr1694 overlaid with the homology model of BlsA. Slr1694 BLUF (PDB: 2HFO). Residue numbering is for BlsA, with the corresponding residues for Slr1694 BLUF in parentheses. H-bonds between the flavin and the protein are depicted by yellow dots and are shown for Slr1694 BLUF. The figure was made using free software Pymol (The Pymol Molecular Graphics System, version 1.5.0.5; Schrödinger, LLC: Portland, OR, 2001).

question on the functionality of BlsA protein at different temperatures (2,15). Indeed, *blsA* transcript levels were found to be lower at 37°C than at 24°C in cells obtained from motility plates (2), suggesting that a point of control would exist at this level. To broaden our understanding of the temperature dependency of BlsA functionality, in this work we have studied *blsA* expression at the transcriptional and protein level, and the potential perturbations in the nanoenvironment of FAD in BlsA by UV–vis absorption and fluorescence spectroscopy at different temperatures. Overall, we provide insights into BlsA functioning by showing that BlsA levels are negligible at 37°C in the bacteria and that the reversible photocycle is mainly operative below 30°C using the purified recombinant protein.

The overall evidences indicate that temperature influences photoregulation at different points, being modulation of BlsA content in the cell a critical aspect at established temperatures, while differential photoactivity of BlsA would be key to restrict photoregulation in the short term, *that is* in sudden temperature changes when the photoreceptor is already present in the cell. In this way, we show that BlsA itself is able to integrate temperature changes with photoactivity.

MATERIALS AND METHODS

Acinetobacter baumannii ATCC 17978 growth curves. To determine *A. baumannii* ATCC 17978 growth curves, 1/100 dilutions of overnight cultures grown in LB (Difco) at 37°C were inoculated in fresh LB media and grown with vigorous shaking under blue light using a nine-LED (light-emitting diode) array with an intensity of 6–10 μEinstein m^{-2} s^{-1} or incubated in the dark, both at 24°C and 37°C. Monitoring of the growth curves was performed by measuring the absorbance at 600 nm of small aliquots of the culture suspension as a function of time.

Transcriptional analysis. Culture aliquots grown as indicated above were extracted at the indicated time points. Cells were pelleted and immediately mixed with 1 mL lysis buffer (0.1 M sodium acetate, 10 mM EDTA, 1% SDS) in a boiling-water bath. Cell lysates were extracted twice at 60°C with one volume of phenol, which was adjusted to pH 4.0 with 50 mM sodium acetate, and then once with chloroform at room temperature. The RNA precipitated overnight at −20°C with 2.5 volumes ethanol was collected by centrifugation, washed with 70% ethanol and dissolved in DEPC-treated deionized water. Total RNA samples were treated with RNase-free DNase I. RNA quality and quantity was evaluated by gel electrophoresis and by determination of the absorbance 260/280 nm relation. Retrotranscription and qRT-PCR analysis were carried out as previously described (16), using primers listed in Table S1 of the Supporting Information. Each cDNA sample was run in technical triplicate and repeated at least two independent sets of samples.

Protein analysis. Overnight cultures of *A. baumannii* ATCC 17978 were pelleted by centrifugation at 10 000 ***g*** for 10 min at 4°C, resuspended in phosphate saline buffer (PBS) [NaCl 137 mM; KCl 2.7 mM; Na_2HPO_4 4.3 mM; KH_2PO_4 1.47 mM (pH 7.4)] and sonically disrupted in the presence of 0.2 mM PMSF. Soluble extracts were obtained from total extracts, by centrifugation at 20 000 ***g*** for 20 min at 4°C. Protein concentration was determined by the Bradford method (17). Soluble proteins were size fractionated by sodium dodecyl sulfate–polyacrylamide gel electrophoresis (SDS-PAGE) using 12.5% polyacrylamide gels and either stained with Coomassie blue or electrotransferred onto nitrocellulose filters (Amersham). The protein blots were probed with anti-BlsA serum, and the secondary antibody used is anti-rabbit conjugated to HRP (BioRad). It should be noted that BlsA levels were found to be low in the cells, which is not surprising given its nature as a regulatory protein (18). We therefore used the Super Signal West Femto Maximum Sensitivity Substrate Trial Kit (Thermo Scientific) to be able to detect the immunocomplexes.

Production of polyclonal antibodies. BlsA was overexpressed and purified as a His-Tag derivative from pET-TEV as described in Mussi *et al.* (2). The purified protein was used to elicit antibodies in rabbits by following procedures described before (19). The antibodies obtained were further affinity purified using nitrocellulose membranes to which BlsA had been electrophoretically attached.

Overexpression and purification of BlsA. BlsA protein from *A. baumanii* ATCC 17978 was overexpressed in *Escherichia coli* BL21 pLys and purified as previously described (2,15) with the exception that the His-tag was not removed from the protein using the TEV protease. Purified protein was conserved at 4°C for over a period of up to 7 days, as freezing caused the loss of the cofactor FAD. Protein concentrations were determined as *holoprotein* using the absorption coefficient of FAD (11.3 mM^{-1} cm^{-1} (20)), and as *total protein* using the absorption coefficient of 19.9 mM^{-1} cm^{-1} at 280 nm, as calculated using the approach of Gill and von Hippel (21) for the aminoacid sequence of BlsA. Apoprotein concentrations were calculated as the difference between total protein minus holoprotein. Blue-light irradiation of BlsA was performed using a Royal Blue LED (Luxeon Star Leds) at 443 ± 20 nm. Light intensity was determined by chemical actinometry using potassium ferrioxalate according to IUPAC Chemical Actinometry (22). Samples were incubated at a given temperature for 10 min, centrifuged at 16 000 ***g*** for an hour to eliminate turbidity and incubated again for 5 min at the desired temperature before any spectroscopic assay was performed.

FAD delivery assay. To evaluate the protein capability to retain FAD, dialysis experiments were performed using a D-tube Midi MWCO 3.5 kDa (Novagen) at 15°C and 37°C. An aliquot of 750 μL of purified solution of dBlsA (13.5 μM) was dialyzed for 3 h (as recommended by the D-tube Midi manufacturer) against 20 mL of buffer solution with constant stirring. All buffers, glass material and dialyzers were kept at the desired temperature for 24 h before adding the protein sample in the D-tube. Inside and outer concentrations of total protein and FAD were analyzed before and after dialysis process by monitoring absorbance at 280 and 450 nm, respectively, using the extinction coefficient values mentioned previously.

A second dialysis procedure at 37°C was performed but dialyzing 1.2 mL of 10.4 μM dBlsA against 1000 mL of buffer with constant starring to assure the full FAD delivery to the buffer solution under larger dilution condition.

Spectroscopic measurements. Absorption spectra were registered using a modular miniature UV–vis spectrophotometer USB2000+ (Ocean Optics, USA), connected via optic fiber to a UV–vis light source (Analytical Instrument System, USA). The assays were carried out using a 5 × 5 mm quartz cuvette (Hellma, Müllheim, Germany) with 350 μL of a fresh BlsA protein, mounted on a FLASH 300 Cuvette Holder

connected to a Peltier based temperature controller (Quantum Northwest). Scattering effects on the absorption spectra were corrected using a|e – UV-Vis-IR Spectral Software 1.2, FluorTools (www.fluortools.com). Fluorescence emission spectra were recorded with a Hitachi F-2500 spectrofluorimeter (Kyoto, Japan) equipped with a Hamamatsu R-928 photomultiplier. A neutral density filter of 10%T was placed onto the excitation output beam to minimize photochemical processes during acquisition. Emission spectra of BlsA were obtained by selective excitation of FAD cofactor at 450 nm. All measurements were registered between 15.6° and 36.6°C in air-saturated protein solution.

Fluorescence lifetimes were registered using a Tempro-01 time-correlated single photon counting (TCSPC) system (Horiba, Glasgow, UK) as described before, as well as the data analysis (23,24). Briefly, the fluorescence intensity decays obtained by excitation with a pulsed blue-LED (Nanoled® 461 ± 27 nm, 1 MHz, Horiba) were fitted with the fluorescence decay analysis software DAS6® (Horiba) by deconvolution of the pulse function (obtained with a diluted Ludox® suspension at the excitation wavelength) using a multiexponential model function (24).

The temperature control of both steady-state and time-resolved fluorescence experiments were performed using a circulating fluid bath (Haake F3) connected to the cuvette holder. All experiments were performed by duplicate and the average values with standard deviation are reported.

RESULTS AND DISCUSSION

blsA is preferentially expressed in the dark at low temperatures

Expression analyses at the transcriptional level show that *blsA* expression is higher in the stationary phase in the dark (D) at 24°C than under illuminated (L) conditions or exponential phase (Fig. 2a). Indeed, *blsA* transcriptional levels analyzed from cell culture samples obtained at different optical densities (representative of different phases of the growth curve), indicated that at 24°C *blsA* levels are higher in the dark relative to illuminated conditions along the exponential phase (Figs. 2a and S1a). However, these values were overall significantly lower than in the stationary phase, particularly in the dark. On the contrary, at 37°C, *blsA* expression levels were markedly lower than at 24°C both at exponential and stationary phases (Figs. 2a and S1b), and similar between light and dark.

Western blot analyses directed against BlsA show that, in agreement with expression analyses at the RNA level, BlsA protein levels are much higher in the dark at 24°C than under blue light in cultures grown to stationary phase (see Fig. 2b). Interestingly, BlsA levels are almost negligible at 37°C both under blue light and in the dark (Fig. 2b).

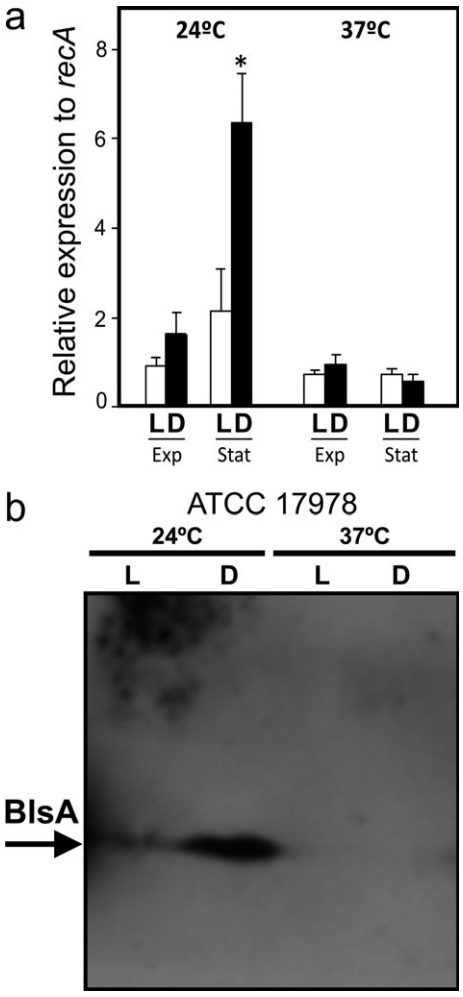

Figure 2. (a) Effects of light and temperature on *blsA* expression. RNA from *Acinetobacter baumannii* ATCC 17978 cells grown at exponential (Exp) or stationary (Stat) phase in LB with vigorous shaking at 24°C and 37°C, in the presence of blue light (L) or in the dark (D), was used as template for qRT-PCR using *blsA* specific primers. *recA* was used as a constitutively expressed internal control. The means ± SD of independent experiments are represented by bars. Asterisk indicates significant differences calculated by the Bonferroni test ($P < 0.05$). (b) Effects of light and temperature on BlsA protein levels. Immunoblot analysis of protein samples from bacteria grown overnight in LB with vigorous shaking at 24°C and 37°C, in the presence of blue light (L) or in darkness (D), using purified antibodies directed against BlsA. Crude extracts corresponding to 350 μg of total proteins were loaded in each lane.

Temperature effect on cofactor–protein interactions and BlsA photocycle

Figure 3a compares the UV–vis absorption and fluorescence spectra of dBlsA at 15.6 and 36.6°C with those of FAD in the working buffer solution (20 mM TRIS, 500 mM NaCl, 1 mM 2-mercaptoethanol, 250 mM imidazole, 4% glycerol, pH 8) at 23.5°C. The shape of the absorption spectra of dBlsA was similar to that reported before, with the two characteristic $\pi \rightarrow \pi^*$ absorption bands of the fully oxidized isoalloxazine ring, corresponding to the transitions from the ground state (S_0) to the lowest lying excited states of the singlet manifold S_1 ($\lambda^{max} \approx 450$ nm) and to the upper S_2 ($\lambda^{max} \approx 360$ nm). As compared with free FAD, in dBlsA, the S_2 band shows stronger hyperchromic effect, as previously reported for this photoreceptor (2,3). More importantly, the S_1 band split into extra vibrational transition bands, displaying a hyperchromic effect at the red edge with a well-defined vibrational shoulder at approximately 485 nm. The raising of vibronic (vibrational + electronic) modes in the $S_0 \rightarrow S_1$ transition of flavin chromophores is the result of less polar, and/or hydrogen-bonding, and/or rigid nanoenvironment around the isoalloxazine ring of the flavins (20). Besides the modifications of the FAD absorption spectra, prolonged heating above 30°C also produces scattering increment of the solution suggesting protein instability.

The fluorescence emission spectra of dBlsA obtained by excitation at 450 nm were blue-shifted compared with that of free FAD (Fig. 3a). The emission band of dBlsA was progressively shifted to the blue as temperature decreased, whereas for the fluorescence emission of free FAD in buffer was almost

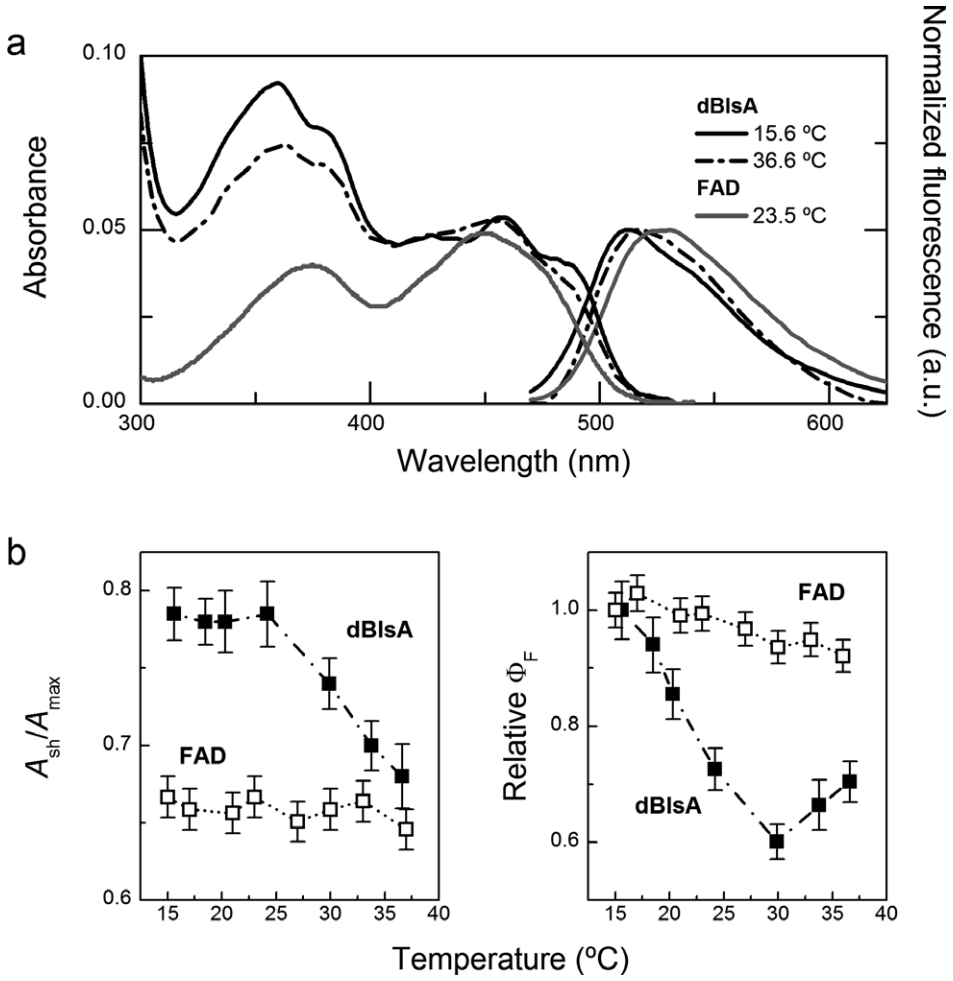

Figure 3. (a) Steady-state UV–vis absorption and emission spectra (λ_{ex} = 450 nm) of dBlsA at different temperatures and of FAD in buffer at 23.5°C. (b) Variation with temperature of the ratio between the absorbance of the vibrational shoulder and maximum (A_{sh}/A_{max}), and of the relative fluorescence quantum yield (Φ_F) for FAD in buffer (□) and in dBlsA (■).

independent of temperature (data not shown). These results confirm that as temperature decreases, the cofactor in dBlsA senses a less polar nanoenvironment than in bulk buffer (20,23).

It has been reported that for FAD-bearing proteins containing Trp and/or Tyr residues at closer distances (<5 Å) to the isoalloxazine ring the absorption band $S_0 \rightarrow S_1$ also shows the hyperchromic effect at the red edge described above (25,26). In the case of BlsA, the conserved Tyr7 is about 4.8 Å from the isoalloxazine ring (Fig. 1), and hence, this should be the case. Thus, the absorbance ratio between the vibrational bands at the red-shoulder and at the maximum, for example A_{sh}/A_{max}, was proposed as convenient parameter to monitor the environmental changes of the nanospace around FAD (23,25). Figure 3b shows that ratio A_{sh}/A_{max} for dBlsA is constant between 15.6 and 24.2°C, but it is strongly decreased at higher temperatures up to a closer value observed for free FAD, being the latter not sensitive to temperature.

Figure 3b also compares the relative changes of fluorescence quantum yield (Φ_F) with temperature of free FAD in buffer and in dBlsA. For free FAD the relative fluorescence quantum yield only fade less than 7% in the studied temperature range, but for dBlsA decreased about 30% at 30°C but above this temperature the fluorescence was partially recovered.

Table 1 shows the fluorescence decay data of FAD obtained by the TCSPC technique and the deconvolution fitting procedure with a multiexponential function to obtain the individual lifetime (τ_i) and fractional contribution (f_i) values of the ith decay component as described before (23,24). The individual lifetime composition of FAD decay in dBlsA was different to that observed both in buffer and neat water. Despite of the complex decay behavior, the average fluorescence lifetime $\langle\tau\rangle = \Sigma f_i\tau_i$ of FAD in dBslA was almost constant between 15.6°C and 24.2°C, but increased at 36.6°C.

Altogether, the spectroscopic properties of dBlsA suggests that heating above 30°C produces conformational modifications in the dark-adapted protein that can result in loss of FAD and protein aggregation. As mentioned before, the ratio A_{sh}/A_{max} can be used to monitor the nanoenvironmental changes around the isoalloxazine ring of the flavin and also the proximity with conserved Tyr and/or Trp residues (23,25). In turn, the Φ_F value of either intrinsic or extrinsic fluorophore in a protein depends on several factors including hydrogen-bonding, intraprotein quenching and local rigidity; all of them strongly depending on the protein conformation, fluorophore orientation and binding strength (27). For dBlsA at T < 25°C, both A_{sh}/A_{max} and $\langle\tau\rangle$ were nearly constant, but the relative Φ_F decreased with temperature (Fig. 3b

Table 1. Fluorescence decay parameters obtained by multiexponential fitting deconvolution of fluorescence decays of FAD in dBlsA, buffer and neat water at different temperatures.

	T (°C)	λ_{em} (nm)	τ_1 (ns)	f_1	τ_2 (ns)	f_2	τ_3 (ns)	f_3	$\langle\tau\rangle$ (ns)	χ^2
dBlsA (buffer)	15.6	510	0.09	0.74	0.89	0.10	9.18	0.16	1.61	1.17
	20.3		0.06	0.74	0.79	0.11	9.09	0.15	1.47	1.17
	24.2		0.08	0.72	0.88	0.14	9.00	0.14	1.44	1.18
	36.6		0.42	0.47	1.82	0.34	8.23	0.19	2.35	1.27
FAD (buffer)	23.5	510	0.74	0.90	1.97	0.10	–	–	0.87	0.99
		540	0.73	0.87	1.71	0.13	–	–	0.86	1.01
FAD (water)	23.5	540	0.156	0.05	2.49	0.49	4.79	0.46	3.43	1.13

and Table 1). In principle, this behavior suggests that the structural conformation of the FAD binding site in dBlsA remained practically relentless but became less rigid with temperature, enhancing nonradiative deactivation processes (k_{nr}) of the S_1 state of FAD in detriment of radiative relaxation (k_F) (27).

On the contrary, heating at $T > 25$°C produced the combined diminution of A_{sh}/A_{max} with the partial recovery of the relative Φ_F (Fig. 3b) and increment of $\langle\tau\rangle$ of FAD in dBlsA at 36.6°C (Table 1). These changes could be the result of temperature-induced conformational modification of the binding site of FAD that produces either a larger separation or different orientation of the isoalloxazine ring with the closer Tyr7, contributing to decreases the efficiency of prompt photoinduced ET from the aromatic residue to the S_1 state of FAD (25,26) or protein denaturalization with release of FAD.

Dialysis experiments performed with a 3.5-kDa-cutoff membrane (Table S2) confirmed that at 15°C the protein remains soluble and 94% of cofactor was retained. Instead, at 37°C about 70% of the total protein was precipitated, but the soluble BlsA fraction contained about 86% of FAD. Thus, at high temperature, a significant fraction of dBlsA suffers a conformational change and aggregate while the remaining soluble fraction is able to retain the cofactor.

Under this framework, the fluorescence lifetime data of Table 1 show that $\langle\tau\rangle$ values of FAD in dBlsA were intermediate of those observed in buffer and neat water, respectively. In fluid solutions, the ultrafast intramolecular electron-transfer quenching process of the S_1 state of the isoalloxazine of FAD by the pendant adenine moiety by coplanar stacking of both aromatic rings is allowed, producing populations of intramolecular conformers between the "closed" (completely quenched) to "open" (unquenched) conformations (28). In the case of FAD in buffer, it can be also expected an extra "impurity" quenching contribution by buffer components. Thus, the increased $\langle\tau\rangle$ of FAD in dBlsA compared with buffer should be a combination of an open conformation FAD into the binding site (Fig. 1) with the presence of free FAD molecules in the buffer solution. The partial release of FAD at 37°C explains the increment of the fluorescence fraction contribution of the intermediate lifetime component, *that is* $\tau_2 \approx 1.8$ ns, while the contribution of about 20% of the longer lifetime, *that is* $\tau_3 \approx 8$ ns confirms that a fraction of the protein retains the cofactor even when conformational changes of dBlsA were produced by heating (Table 1).

Figure 4a shows the UV–vis absorption spectral changes elicited after 500 s of steady-state illumination with a blue-LED emitting at 443 nm of dBlsA at 15.6°C. As shown in previous reports, a red-shift of ≈10 nm the absorption maximum was observed assigned to the formation of the signaling state sBlsA (2,3). Ultra-fast transient spectroscopy studies of BlsA (3) and of other related BLUF proteins (6,10,13,14) demonstrated that the formation of BLUF signaling state produces the flip of the conserved Gln residue together with the reinforcement of the hydrogen-bonding network. Thus, these conformational changes are responsible of the UV–vis absorption spectral changes observed.

The differential absorption spectrum showed a well-defined band at 510 nm, whose amplitude decreased with temperature (lower panel of Fig. 4a), suggesting that the amount of sBlsA was strongly reduced at high temperature. The red-shift of the absorption maximum ($\Delta\lambda_{max}$) produced during photoactivation of dBlsA was also smaller with the temperature increment, being very small at 36.6°C (Fig. 4b). This figure also shows that the temperature dependence of the ratio A_{sh}/A_{max} for sBlsA was similar to that observed for the dBlsA state (Fig. 3b), with a constant value between 15.6–24.2°C and decreasing above 25°C (Fig. 4b).

Figure 4c shows the kinetic curve monitored at 510 nm for the formation of sBlsA upon blue-LED illumination of dBlsA at 15.6°C, followed by a slower decay under darkness to the dBlsA state, which was subsequently illuminated again. Similar kinetic behavior was only reproduced at $T < 30$°C. Above this temperature, the kinetic trace at 510 nm was fluctuating within the signal-to-noise ratio of the spectrometer (Fig. S2). Hence, the apparent first-order rate constants (k) for the photoactivation and dark recovery of dBlsA were obtained only in the temperature range of 15.6°C and 24.2°C by exponential fitting (gray solid lines in Fig. 4d) of the growth and decay kinetic profiles, respectively, and those values are reported in Table S3. By plotting the k values according to the classical Eyring's equation, the activation enthalpy and entropy values of each process were obtained, for example $\Delta H^{\ddagger} = 13 \pm 2$ kJ mol^{-1} and $\Delta S^{\ddagger} = -240 \pm 30$ J K^{-1} mol^{-1} for the photoactivation of dBlsA; and $\Delta H^{\ddagger} = 50 \pm 5$ kJ mol^{-1} and $\Delta S^{\ddagger} = -117 \pm 10$ J K^{-1} mol^{-1} for the thermal decay of sBlsA (Fig. 4d).

Comparing the activation parameters one can assume that the photoactivated formation of sBlsA requires four-fold less activation enthalpy than for dark relaxation to the dBlsA state. Thus, from this state the apparent activation energy of formation of the sBlsA at room temperature, $E_a = \Delta H^{\ddagger} + RT = 16 \pm 2$ kJ mol^{-1}, was similar to the activation barrier (<20 kJ mol^{-1}) of the "butterfly" bending motion in the isoalloxazine ring produced during the reduction of oxidized flavin (planar) to reduced flavin (bent) (29). Upon excitation of dBlsA, the energy gain of the relaxed excited state S_1 state of the cofactor is approximately 241 kJ mol^{-1}; calculated from the wavelength crossing between the normalized absorption and emission spectra (Fig. 3a). Hence, the obtained $E_a \approx 16$ kJ mol^{-1} could be assigned to the

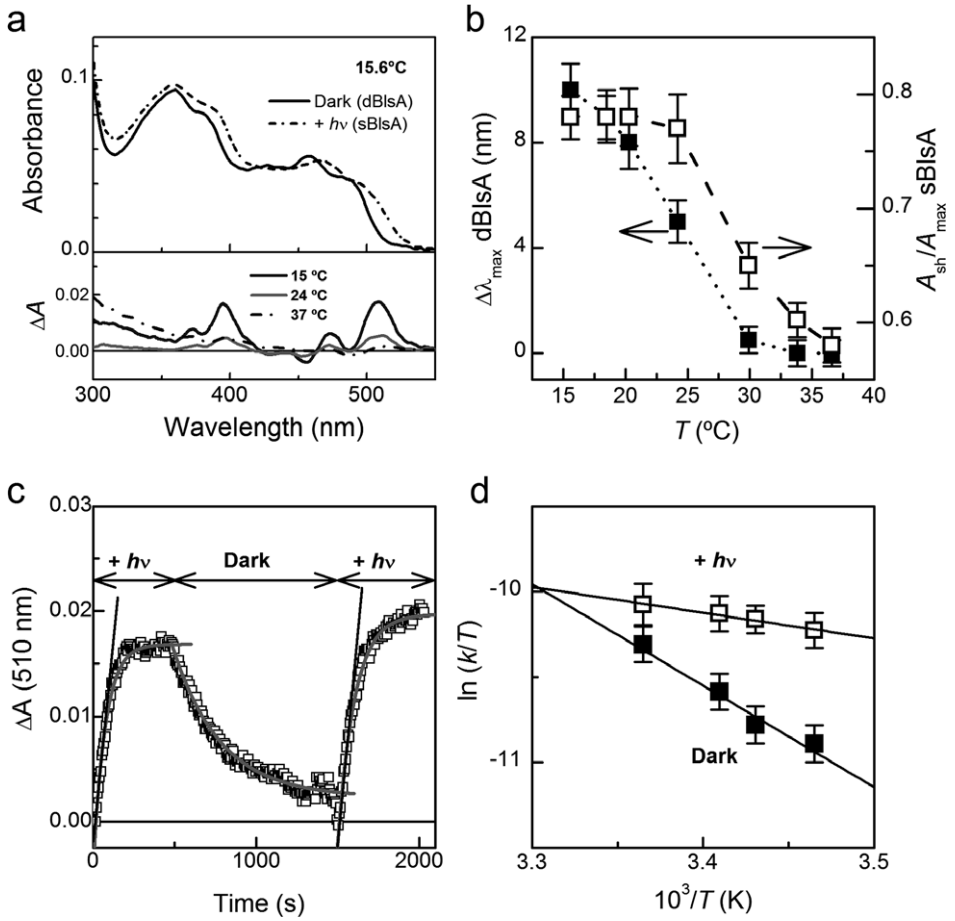

Figure 4. (a) Steady-state UV–vis absorption changes produced after 500 s of blue-LED (443 ± 20 nm) illumination of dBlsA (solid line) to produce the signaling state sBlsA (dash-dot line) at 15.6°C. (b) Differential UV–vis absorption spectra after blue-LED illumination at different temperatures. (c) Kinetic profile at 15.6°C of absorbance changes at 510 nm observed for the blue-light photoactivation and dark recovery of BlsA. (d) Eyring's plots for the photoactivation (□) and dark recovery (■) of BlsA.

activation barrier for the formation of FAD radical anion ($FAD^{\cdot -}$) followed of the generation of the neutral flavin semiquinone FADH radical ($FADH^{\cdot}$) due to the ultrafast electron transfer and subsequent proton transfer from a nearby Tyr residue, for example Tyr7 in BlsA (6). Furthermore, the photoactivation process to form sBlsA is accompanied by a large reduction of activation entropy, for example $\Delta S^{\ddagger} = -240 \pm 30$ J K^{-1} mol^{-1}. This significant loss of entropy suggests that the formation of the sBlsA is accompanied by internal and external conformational rearrangements. In fact, ultrafast and steady-state infrared spectroscopy revealed that photoactivation of dBlsA induces loss of hydrogen-bonding interactions of the C2 = O of FAD and changes of the β-sheet structure of the protein, particularly, the β5 strand, that are fundamentally different from those observed in other BLUF proteins and that are proposed to be directly relevant to the light-activated function in *A. baumannii* (3).

For the dark relaxation of sBlsA → dBlsA, the observed value of activation entropy also suggests that the process is accompanied by a significant protein conformational rearrangement. However, the recovery to the dBlsA state was accompanied by larger activation enthalpy and lower entropy than the photoinduced formation of sBlsA, suggesting the occurrence of an enthalpy–entropy compensation phenomena (28,30), which is caused by the energy shift produced by the displacement of the hydrogen-bonding network and/or unfolding–refolding processes occurred during the photocycle of the photoreceptor. As driven by temperature, the entropic component compensates the activation free energy, *that is* $\Delta G^{\ddagger} = \Delta H^{\ddagger} - T\Delta S^{\ddagger}$, and the plots of $\Delta G^{\ddagger}$ *vs* T for both photoinduced ($h\nu$) and dark processes shows an intersection at 305 K (32°C), where the same $\Delta G^{\ddagger} = 86 \pm 4$ kJ mol^{-1} is achieved (Fig. S3). Hence, below the observed isokinetic temperature, *that is* $T_{ik} = 32$°C, $\Delta G^{\ddagger}_{h\nu} < \Delta G^{\ddagger}_{dark}$ whereas the opposite occurs above that temperature. Thus, this result suggests that above T_{ik} the activation barrier for the photoactivation of dBlsA is thermodynamically unfavorable as compared with that for dark recovery. As well as the enthalpy–entropy compensation is a ubiquitous phenomenon in supramolecular and macromolecular systems in solution, and many times arises by trivial statistical factors (28,31), in the present case it can be plausible as T_{ik} is larger than the tested temperature range (15.6–24.2°C) (31). Finally, the activation free energy for the dark recovery of BlsA at T_{comp} of 86 kJ.mol^{-1} was similar to $\Delta G^{\ddagger} = 81$ kJ mol^{-1} reported of Tll0078 from *Thermosynechococcus elongatus* BP-1 (5), but much larger than for the blue sensor BlrB of *Rhodobacter sphaeroides, for example* $\Delta G^{\ddagger} = 2.3$ kJ mol^{-1} (12).

The initial rate of the kinetic growth monitored by differential absorbance changes at 510 nm (black straight lines in Fig. 4c)

represents the initial rate of formation of sBlsA. For each tested temperature, similar rate values were obtained for two consecutive photoactivation processes indicating the reversibility of the photocycle after dark recovery, as shown in Fig. 4c for the trace at 15.6°C. The apparent quantum yield of formation of sBlsA state (Φ_{sBlsA}) was estimated following a similar methodology proposed by Fukushima *et al.* (5), but considering the same absorption coefficient of FAD in dBlsA and sBlsA at 455 nm than in water (ε_{455} = 11.3 mM^{-1} cm^{-1} (20)). Thus, the molar absorption coefficient at 510 nm of 1900 cm^{-1} M^{-1} and 5700 cm^{-1} M^{-1} for dBlsA and sBlsA, respectively (Fig. S4). Therefore, the difference molar absorption coefficient at 510 nm was estimated as 3800 cm^{-1} M^{-1}. The incident photon flux of 1.30 nmol s^{-1} was determined by chemical actinometry with potassium ferrioxalate (22), and considering the fraction of absorbed light by FAD in dBlsA samples and the initial rates, Φ_{sBlsA} values of 0.22 ± 0.05 and 0.17 ± 0.07 were calculated at 15.6°C and 24.2°C, respectively. These apparent quantum yields of formation of sBlsA were similar to 0.29 ± 0.03 and 0.24 ± 0.07 reported for the formation of the signaling state of the related BLUF sensors Tll0078 (5) and AppA (14), respectively, but lower than 0.52 reported for PapB (13).

Dialysis experiments (Table S2) discussed above confirmed that after heating at 36.6°C only 30% of the BlsA remained soluble. After cooling at back at 15.6°C this recovered dBlsA was able to respond to blue-light stimuli to form the signaling state sBlsA, which under dark conditions also relaxes back to the dBlsA state as it is shown in Fig. 5. Therefore, the photoactivity of BlsA is completely governed by temperature-dependent conformational changes of the protein, producing a strong reduction of the efficiency of photoactivation and also protein aggregation at temperatures above 30°C.

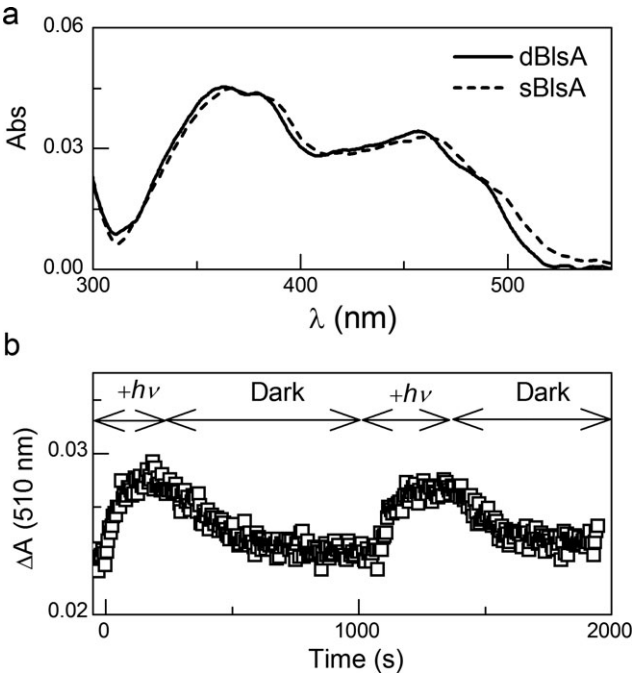

Figure 5. (a) Steady-state UV–vis absorption changes produced after illumination with blue-LED of dBlsA (solid line) to produce the signaling state sBlsA (dash-dot line) at 15.6°C, after recovering of heated protein at 36.6°C (see text). (b) Kinetic profile at 15.6°C of absorbance changes at 510 nm observed for the blue-light photoactivation to sBlsA state and its dark back to dBlsA of the recovered soluble protein after heating at 36.6°C.

CONCLUSIONS

Getting insights into the mechanism of BlsA functioning would provide clues into the mechanism of photoregulation in *A. baumannii,* which governs important traits related to bacterial persistence in the environment and virulence (2).

In this work, we have combined physiological as well as biophysical evidence to begin to understand the basis of the differential photoregulation observed at different temperatures in *A. baumannii* (2). First, we show that *blsA* expression is dependent on the growth phase at 24°C, with higher expression at higher optical densities, perhaps reflecting stages at which phototosensing is important during bacterial life, and also suggesting an induction in response to quorum (quorum sensing). It is also interesting to note that BlsA levels are higher in the dark than under blue light at this temperature, and this could constitute a cellular strategy for optimizing the light sensing machinery to be able to detect any possible appearance of light in the dark condition. Second, *blsA* expression is reduced at 37°C, which correlates with negligible photoreceptor levels in the cells, likely accounting for absence of photoregulation at this temperature. This control of photoregulation seems to be particularly important when the bacteria are adapted to a particular temperature and therefore expression and synthesis of the photoreceptor are also accordingly adapted to the particular condition. Third, we propose that another point of control occurs on the functionality of the photocycle occurring at BlsA itself at different temperatures, which is basically inoperative at temperatures above 30°C. Indeed, spectroscopic and dialysis analyses performed with the purified recombinant protein confirmed that an important fraction of BlsA aggregates, and photoactivation of the remaining soluble fraction does not occur efficiently at higher temperatures, even when the cofactor remains anchored to the protein, but probably with different orientation and/or distance that preclude the photoinduced ET from conserved Tyr7 and therefore the signal transduction. The activation parameters of both processes of the photocycle of BlsA indicate that the protein conformational changes governed by temperature induce enthalpy–entropy compensation effect with isokinetic temperature at 32°C, where the activation free energy of photoactivation becomes larger than for the dark recovery. Hence, it can be expected that dBlsA loses its ability to respond to blue light at temperatures above 30°C. Most interestingly, if temperature of the soluble fraction of BlsA is switched back from 37°C to 15°C, the protein regains ability to respond to blue light by forming the signaling state sBlsA and relaxing back to dBlsA in the dark, that is recovering BLUF activity. This information therefore indicates that modulation by temperature of the BlsA photocycle is reversible implying that this BLUF protein integrates both light as well as temperature information.

Alteration of the photocycle at temperatures above 30°C would then be a third control point occurring at the level of the photoreceptor already present in the cell to avoid almost instantaneously the signaling process when it is no longer necessary, under circumstances of temperature changes possibly faced by the bacteria. For example, if the bacteria are growing at environmental temperatures where photoregulation seems to be important, BlsA is present and active as a photoreceptor. However, if

temperature increases significantly such as in the human host where photoregulation seems not to be important, the BlsA protein already synthesized and present in the cells loses the ability to perform the photocycle and therefore sensing light. One possibility would be that it can then be tagged and directed to degradation, as suggested by the negligible levels of both *blsA* transcript and protein levels observed at 37°C. However, a negligible amount of BlsA, not detectable by our methods, could rest soluble in the cell and regain ability to respond to light in case temperatures lower again. If this low temperature is maintained, then *blsA* transcript and protein levels would then raise again as a result of synthesis *de novo*. All this biophysical and physiological information is summarized in a working model depicted in Fig. 6.

A BLUF domain has already been hypothesized to be a temperature sensor. Tschowry *et al.* showed that the *ycgF* gene from *E. coli*, which is a BLUF domain, is strongly induced at low temperatures and they showed that blue light, cold and starvation are integrated in the expression and activity of YcgF, YcgE (Mer-like repressor) and eight small proteins signaling pathway modulating biofilm formation when *E. coli* has to survive in aquatic environments. Later, Nakasone *et al.* using transient grating measurements showed that YcgF has a photochemistry strongly dependent on temperature. They explained that the nature of these observations is based on a temperature-dependent equilibrium between the monomeric and the dimeric forms of YcgF, with only the monomer being capable to react to blue light and to form dimers, promoting the idea that YcgF could have a biological function as a blue-light and temperature sensor.

Another aspect still to be explored is why does *A. baumannii* photoregulate at environmental temperatures but not at temperatures compatible with warm-blooded hosts. In this sense, it has already been shown that photoregulation occurs at higher temperatures such as 37°C in other members of the *Acinetobacter* genus (15). The fact that these species harbor more than one BLUF-type photoreceptor, accounting for even six in some species such

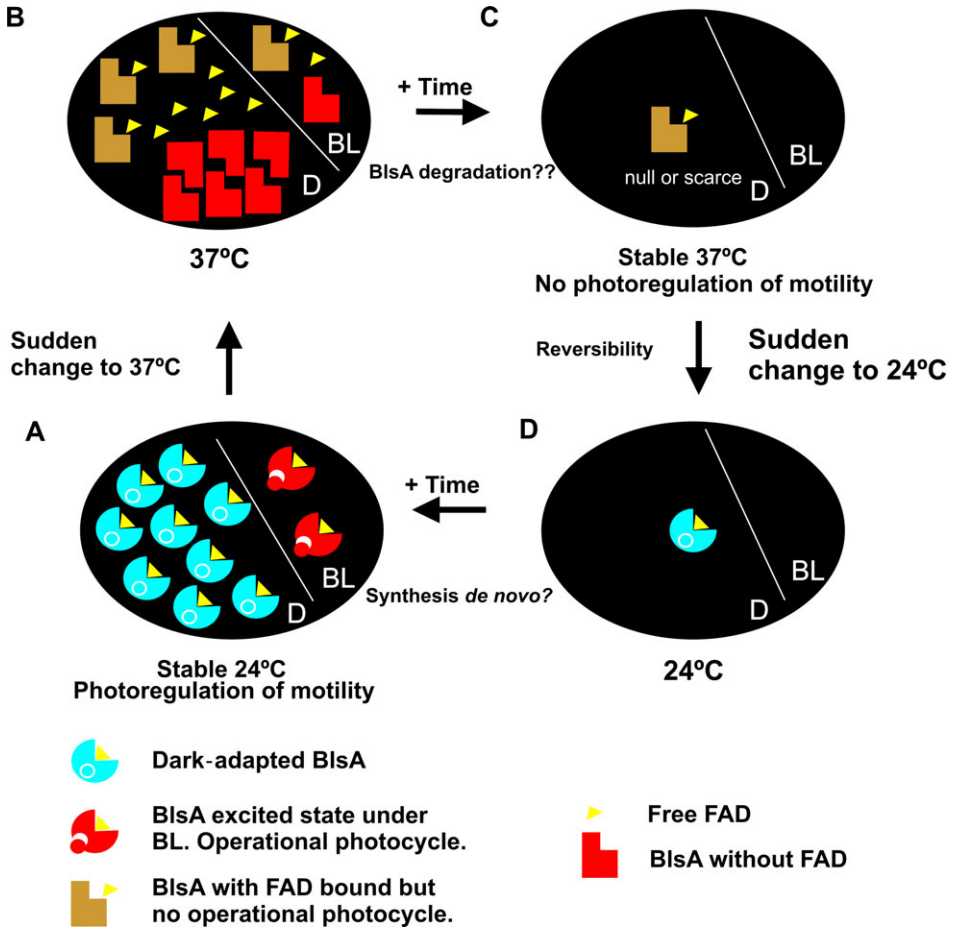

Figure 6. Working model integrating information obtained from physiological as well as biophysical data, to explain the differential response to light observed at different temperatures in *Acinetobacter baumannii*. BL, blue-light and D, dark. BlsA levels under BL or in the dark are represented schematically, according to transcriptional and immunoblot data. It should be noted that overall BlsA levels are low in the cell. Stage A. At 24°C, BlsA enters an excited state changing its conformation and performing the photocycle under blue light. This allows BlsA to interact with partner/s possibly different than those in the dark, displaying thus a differential physiological response. For example, in *A. baumannii* ATCC 17978 at 24°C, the cells move in the dark while are immobile at the inoculation point under blue light. Stage B. Temperature changes to 37°C. A fraction of BlsA molecules lose FAD and aggregate (B), possibly being degraded. Another fraction keeps FAD bound, but performs no photocycle (B and C). No photoregulation of motility occurs. Stage C. After some time at 37°C, the cell harbors almost null levels of BlsA, supporting the hypothesis that BlsA is degraded at this condition. However, a negligible amount of BlsA with bounded FAD could still rest in the cell. Stage D. Temperature changes to 24°C. Reversibility: BlsA is again capable of performing the photocycle. *de novo* synthesis of *blsA* could occur leading again to photoregulation (A).

as *A. radioresistens*, belonging to different monophyletic clusters than BlsA with differences characteristics raise the possibility that these photoreceptors can perceive light at higher temperatures. This possibility is also under study in our laboratories.

Acknowledgements—This work has been supported in part by grants from Agencia Nacional de Promoción Científica y Tecnológica de Argentina (PICT 2012-2666, PICTO-UNSE 2012-0013, PICT 2013-0018 and PICT 2014-1161). I.A., F.E.M.V., M.A.M., G.L.M. and C.D.B. are career researchers of Consejo Nacional de Investigaciones Científicas y Técnicas de Argentina (CONICET). M.C., A.E.G. and P.C.J. are fellows from the same institution.

SUPPORTING INFORMATION

Additional Supporting Information may be found in the online version of this article:

Figure S1. Growth curves of *A. baumannii* ATCC 17978 cells grown in LB media under blue light (open circles) or in the dark (closed circles) at 24 (a) or 37°C (b), are indicated at the right axis. Also indicated in the left axis of the same figures are *blsA* expression patterns at different optical densities (OD) under blue light (open squares) or in the dark (closed squares) at 24 (a) or 37°C (b).

Figure S2. Kinetic profile at 36.6°C of absorbance changes at 510 nm observed for BlsA. Note absorption changes are within the spectral resolution of experimental setup.

Figure S3. Isokinetic plot with a crossing point at 32°C for the variation of the activation free energy as function of temperature for the photoactivated (dBlsA + $h\nu$ → sBlsA) and dark recovery (sBlsA → dBlsA) processes.

Figure S4. UV–vis spectra normalized at the maximum (ε = 11.3 mM^{-1} cm^{-1}) of the $S_0 \rightarrow S_1$ absorption band of the dark (dBlsA)- and blue-light (sBlsA)-adapted species.

Table S1. Primers used in this study.

Table S2. Dialysis data performed during 3 h with D-tube Midi MWCO 3.5 kDa (Novagen) using small volume (sv)[a] and large volume (lv)[a] of exchange buffer.

Table S3. Observed lifetimes for the blue-light-induced and dark recovery of BlsA at different temperature**.**

REFERENCES

1. Spellberg, B. and R. A. Bonomo (2014) The deadly impact of extreme drug resistance in *Acinetobacter baumannii*. *Crit. Care Med.* **42**, 1289–1291.
2. Mussi, M. A., J. A. Gaddy, M. Cabruja, B. A. Arivett, A. M. Viale, R. Rasia and L. A. Actis (2010) The opportunistic human pathogen *Acinetobacter baumannii* senses and responds to light. *J. Bacteriol.* **192**, 6336–6345.
3. Brust, R., A. Haigney, A. Lukacs, A. Gil, S. Hossain, K. Addison, C.-T. Lai, M. Towrie, G. M. Greetham, I. P. Clark, B. Illarionov, A. Bacher, R.-R. Kim, M. Fischer, C. Simmerling, S. R. Meech and P. J. Tonge (2014) Ultrafast structural dynamics of BlsA, a photoreceptor from the pathogenic bacterium *Acinetobacter baumannii*. *J. Phys. Chem. Lett.* **5**, 220–224.
4. Stelling, A. L., K. L. Ronayne, J. Nappa, P. J. Tonge and S. R. Meech (2007) Ultrafast structural dynamics in BLUF domains: Transient infrared spectroscopy of AppA and its mutants. *J. Am. Chem. Soc.* **129**, 15556–15564.
5. Fukushima, Y., K. Okajima, Y. Shibata, M. Ikeuchi and S. Itoh (2005) Primary intermediate in the photocycle of a blue-light sensory BLUF FAD-protein, Tll0078, of *Thermosynechococcus elongatus* BP-1. *Biochemistry* **44**, 5149–5158.
6. Gauden, M., I. H. M. van Stokkum, J. M. Key, D. C. Lührs, R. van Grondelle, P. Hegemann and J. T. M. Kennis (2006) Hydrogen-bond switching through a radical pair mechanism in a flavin-binding photoreceptor. *Proc. Natl Acad. Sci. USA* **103**, 10895–10900.
7. Masuda, S. (2013) Light detection and signal transduction in the BLUF photoreceptors. *Plant Cell Physiol.* **54**, 171–179.
8. Zirak, P., T. Penzkofer, T. Schiereis, P. Hegemann, A. Jung and I. Schlichting (2006) Photodynamics of the small BLUF protein BlrB from *Rhodobacter sphaeroides*. *J. Photochem. Photobiol.* **83**, 180–190.
9. Brust, R., A. Lukacs, A. Haigney, K. Addison, A. Gil, M. Towrie, I. P. Clark, G. M. Greetham, P. J. Tonge and S. R. Meech (2013) Proteins in action: Femtosecond to millisecond structural dynamics of a photoactive flavoprotein. *J. Am. Chem. Soc.* **135**, 16168–16174.
10. Iwata, T., A. Watanabe, M. Iseki, M. Watanabe and H. Kandori (2011) Strong donation of the hydrogen bond of tyrosine during photoactivation of the BLUF domain. *J. Phys. Chem. Lett.* **2**, 1015–1019.
11. Bonetti, C., M. Stierl, T. Mathes, I. H. M. van Stokkum, K. M. Mullen, T. A. Cohen-Stuart, R. van Grondelle, P. Hegemann and J. T. M. Kennis (2009) The role of key amino acids in the photoactivation pathway of the *Synechocystis* Slr1694 BLUF domain. *Biochemistry* **48**, 11458–11469.
12. Wu, Q., W.-H. Ko and K. H. Gardner (2008) Structural requirements for key residues and auxiliary portions of a BLUF domain. *Biochemistry* **47**, 10271–10280.
13. Fujisawa, T., S. Takeuchi, S. Masuda and T. Tahara (2014) Signaling-state formation mechanism of a BLUF protein PapB from the purple bacterium *Rhodopseudomonas palustris* studied by femtosecond time-resolved absorption spectroscopy. *J. Phys. Chem. B* **118**, 14761–14773.
14. Gauden, M., S. Yeremenko, W. Laan, I. H. M. van Stokkum, J. A. Ihalainen, R. van Grondelle, K. J. Hellingwerf and J. T. M. Kennis (2005) Photocycle of the flavin-binding photoreceptor AppA, a bacterial transcriptional antirepressor of photosynthesis genes. *Biochemistry* **44**, 3653–3662.
15. Golic, A., M. Vaneechoutte, A. Nemec, A. M. Viale, L. A. Actis and M. A. Mussi (2013) Staring at the cold Sun: Blue light regulation is distributed within the genus *Acinetobacter*. *PLoS One* **8**, e55059.
16. Ramírez, M. S., G. Traglia, J. Pérez, G. Müller, F. Martínez, A. Golic and M. A. Mussi (2015) White and blue light induce reduction in susceptibility to minocycline and tigecycline in *Acinetobacter sp.* and other bacteria of clinical importance. *J. Med. Microb.* **64**, 525–537.
17. Bradford, M. M. (1976) A rapid and sensitive method for the quantitation of microgram quantities of proteins utilizing the principle of protein-dye binding. *Anal. Biochem.* **72**, 248–254.
18. Aguilar, P. S., A. M. Hernandez-Arriaga, L. E. Cybulski, A. C. Erazo and D. de Mendoza (2001) Molecular basis of thermosensing: A two-component signal transduction thermometer in *Bacillus subtilis*. *EMBO J.* **20**, 1681–1691.
19. Mussi, M. A., A. S. Limansky, V. Relling, P. Ravasi, A. Arakaki, L. A. Actis and A. M. Viale (2011) Horizontal gene transfer/assortative recombination within the *Acinetobacter baumannii* clinical population provides genetic diversity at the single carO gene encoding a major outer membrane protein channel. *J. Bacteriol.* **193**, 4736–4748.
20. Heelis, P. F. (1982) The photophysical and photochemical properties of flavins (isoalloxazines). *Chem. Soc. Rev.* **11**, 15–39.
21. Gill, S. C. and P. H. von Hippel (1989) Calculation of protein extinction coefficients from amino acid sequence data. *Anal. Biochem.* **182**, 319–326.
22. Kuhn, H. J., S. E. Braslavsky and R. Schmidt (2004) Chemical actinometry (IUPAC Technical Report). *Pure Appl. Chem.* **76**, 2105–2146.
23. Valle, L., I. Abatedaga, F. E. M. Vieyra, A. Bortolotti, N. Cortez and C. D. Borsarelli (2015) Enhancement of photophysical and photosensitizing properties of flavin adenine dinucleotide by mutagenesis of the C-terminal extension of a bacterial flavodoxin reductase. *ChemPhysChem* **16**, 872–883.
24. Valle, L., F. E. M. Vieyra and C. D. Borsarelli (2012) Hydrogen-bonding modulation of excited-state properties of flavins in a model of aqueous confined environment. *Photochem. Photobiol. Sci.* **11**, 1051–1061.

25. Mataga, N., H. Chosrowjan, Y. Shibata, F. Tanaka, Y. Nishina and K. Shiga (2000) Dynamics and mechanisms of ultrafast fluorescence quenching reactions of flavin chromophores in protein nanospace. *J. Phys. Chem. B* **104**, 10667–10677.
26. van den Berg, P. A. W., A. van Hoek, C. D. Walentas, R. N. Perham and A. Visser (1998) Flavin fluorescence dynamics and photoinduced electron transfer in Escherichia coli glutathione reductase. *Biophys. J* . **74**, 2046–2058.
27. Lakowicz, J. R. (2006) *Principles of Fluorescence Spectroscopy*. Springer Science+Business Media, LLC, Singapore.
28. Liu, L. and Q.-X. Guo (2001) Isokinetic relationship, isoequilibrium relationship, and enthalpy-entropy compensation. *Chem. Rev.* **101**, 673–695.
29. Moonen, C. T. W., J. Vervoort and F. Mueller (1984) Carbon-13 nuclear magnetic resonance study on the dynamics of the conformation of reduced flavin. *Biochemistry* **23**, 4868–4872.
30. Borsarelli, C. D. and S. E. Braslavsky (1998) Volume changes correlate with enthalpy changes during the photoinduced formation of the ^{3}MLCT) state of ruthenium(II) bipyridine cyano complexes in the presence of salts. A case of the entropy-enthalpy compensation effect. *J. Phys. Chem. B* **102**, 6231–6238.
31. Sharp, K. (2001) Entropy—enthalpy compensation: Fact or artifact? *Protein Sci.* **10**, 661–667.